

The Quantum Mechanics of Alpha Decay

Lulu Liu (Partner: Pablo Solis)*
 MIT Undergraduate
 (Dated: December 9, 2007)

We verify the empirical Geiger-Nuttall relationship, and simultaneously Gamow's model of alpha decay, which predicts a linear relation between the log of the observed half-life of alpha emitters and inverse of the square root of its alpha energy. The energies and half-lives of several alpha-emitting isotopes are determined through judicious use of the equipment at hand, including photomultipliers, counters, solid-state detectors, time-to-amplitude converters, and coincidence circuitry. In the end, six half-lives were determined. We find the half-lives of Rn^{222} , Po^{218} , Po^{214} , Po^{212} , Bi^{211} , and Bi^{212} to be 3.86 ± 0.41 days, 188.4 ± 19.8 s, 163.7 ± 13.1 μ s, 0.31 ± 0.01 μ s, 2.17 ± 0.18 min, and 67.8 ± 7.8 min, respectively.

1. INTRODUCTION

Alpha decay has been a source of confusion for classical physicists for quite some time. According to classical theory, a positively charged alpha particle encounters a repulsive potential near the nucleus of an atom, $V(r) = Z_n Z_\alpha e^2 / r$ (where $Z_n e$ is the charge of the daughter nucleus and $Z_\alpha e$ is the charge of the alpha particle), which ends abruptly (to a decent approximation) at the radius of the nucleus, R_0 . The minimum energy necessary for an alpha particle to escape from the nucleus can then be found by evaluating the potential at its local maximum, $r = R_0$. This minimum energy is high enough that we should, in theory, see almost no spontaneous alpha emission, however, this is not what we observe. In fact, not only is alpha emission a frequent occurrence in nature, the energies of these alpha particles emitted are several times smaller than the predicted energy minimums. It became obvious that classical theory was inadequate in describing the physics of nuclear decay events. In addition, classical physics offered no explanation for the incredible range of half-lives of particles decaying via alpha emission, which extends from less than a microsecond to trillions of years, over many orders of magnitude.

2. QUANTUM TUNNELING AS A MODEL

Quantum mechanics offers an alternative description. A particle partially bound within a finite potential well has a certain probability, upon each encounter with the barrier, of appearing as a free particle on the other side, see Figure 1. This probability is known as the transmission coefficient, T , and can be determined roughly using WKB approximation [1].

$$T = \exp\left(-\frac{2}{\hbar} \int_{R_0}^{r_1} (2m|E - V(r)|)^{1/2} dr\right) \quad (1)$$

where R_0 is the atomic radius, E is the energy of the

alpha particle, and r_1 is the radius at which $E = V(r)$. Following the derivation in [1], one arrives at a relation between the half-life of an alpha decay process and the energy of the emitted alpha particles,

$$\ln(1/\tau_{1/2}) = a_1 \frac{Z_n}{\sqrt{E}} + a_2 \quad (2)$$

where $\tau_{1/2}$ is the half-life and a_1, a_2 are constants. This equation was originally derived by Gamow in his 1928 paper, but previously had been found empirically by Geiger and Nuttall in the form $\ln(1/\tau) = a_1 \ln(E) + a_2$. In verifying the Geiger-Nuttall Law, we hope to show quantum mechanics as the prevailing theory for interactions on an atomic scale.

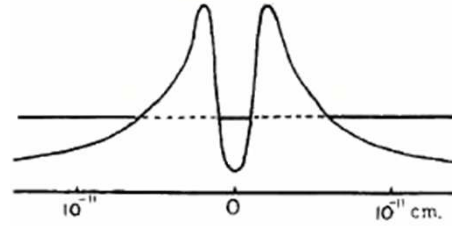


FIG. 1: Approximation of the repulsive potential seen by an alpha particle, with the center of the nucleus at $r = 0$.

3. NATURALLY RADIOACTIVE SERIES AND THE BATEMAN EQUATIONS

Isotopes of importance to us come from the three naturally radioactive series. Since isolated observation is impossible under our conditions, it becomes important to model the activity of any member of a decay chain under certain initial conditions. We invoke the solutions to the Bateman differential equations, which govern the time evolution of all elements in a radioactive chain. The basic concept is illustrated using a two-element decay chain where A represents the abundance of the first element,

*Electronic address: lululu@mit.edu

which decays into B .

$$dA/dt = -A/\tau_A \quad (3)$$

$$dB/dt = A/\tau_A - B/\tau_B \quad (4)$$

This can be extended to decay chains with many elements, and can be solved numerically or analytically to produce results such as follows, which is used to predict the rate of alpha particles emitted:

$$A(t) = A_0 e^{-t/\tau_A} \quad (5)$$

$$B(t) = B_0 e^{-t/\tau_B} + A_0 \frac{\tau_B}{\tau_A - \tau_B} \left(e^{-t/\tau_A} - e^{-t/\tau_B} \right) \quad (6)$$

4. EQUIPMENT

Various apparatus were used in our experiment, most frequently is a set-up involving a metal can containing rocks of many isotopes of uranium, Figure 2. This apparatus allows us to observe all radioactive decay events following the production of polonium from radon gas.

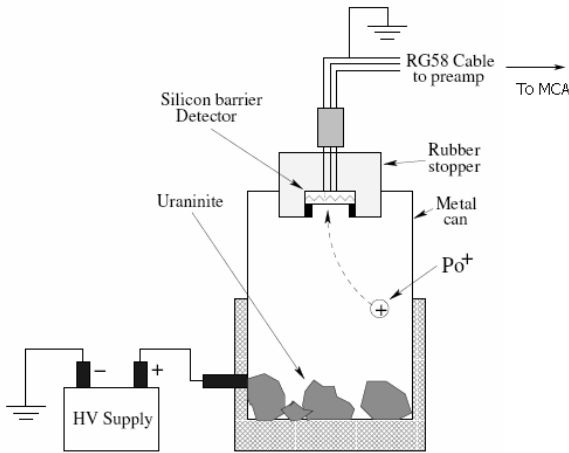


FIG. 2: Metal can containing uraninite. A bias voltage may be applied between the top and bottom of the can to draw ionized polonium decay products into the solid state detector in the lid. The output is fed to an MCA which bins the radiation detected according to energy.

5. MEASURING ENERGIES

The energies of all isotopes of interest were derived from measurements using the can-detector-MCA set up. Single-point calibration was made by associating the highest energy peak with the known energy of Po^{212} , at 8.78 MeV. All peaks were then identified by their relative heights and positions on the energy spectrum by referencing [2].

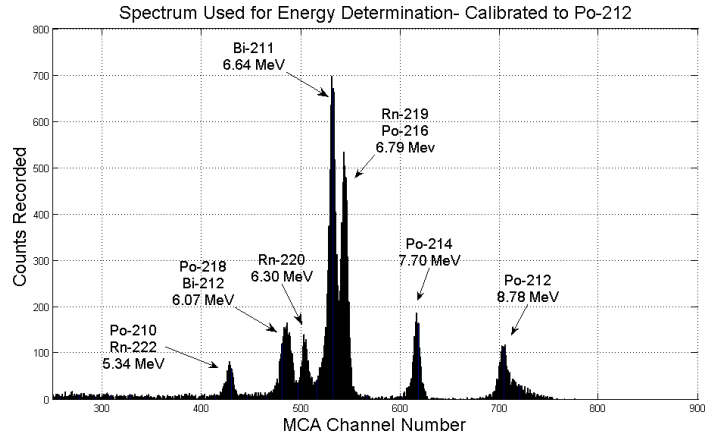


FIG. 3: Energy spectrum of alpha particles emitted by identified isotopes. Voltage is applied between the top and bottom of can.

6. MEASURING HALF-LIVES

6.1. Rn^{222} Half-Life Using the Liquid Scintillator

We inject a vial of liquid scintillating fluid with a sample of Rn^{222} prepared from a radon farm of uranite rocks. The vial is then lowered into a coincidence circuit of two photomultiplier tubes which feed a counter used to tally the total activity in the vial at a given time.

Using the bateman relations, we obtain a model of the expected total rate, as shown in Figure 4. An initial abundance of pure radon is assumed, and we see a rise time in total activity on the order of hours. To obtain measurements representative of the half-life of Rn^{222} , it was necessary that the first measurement occur when a pseudo-equilibrium state has been established in which all active isotopes are decaying at the rate of Rn^{222} .

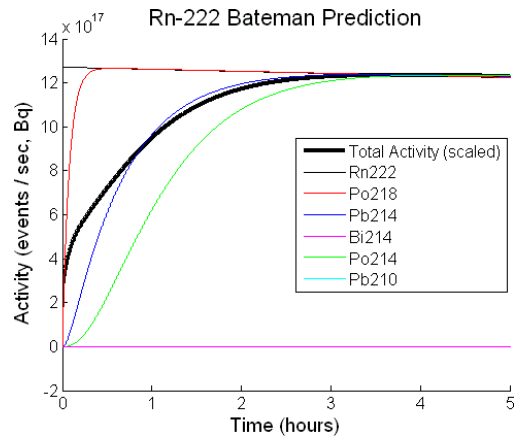


FIG. 4: Rise time of activity of Rn^{222} and its decay products in the liquid scintillator.

Background was taken along with each of our measurements using a vial of only scintillator fluid and found to be in general 1 /s. With repeated trials limiting our er-

ror, the results of our half-life determination for Rn^{222} is shown in Figure 5 with background subtracted. We were able to fit an exponential with a $\chi^2_{\nu-1}$ of 2.6 and half-life of 3.99 ± 0.36 days. The accepted value from [3] is 3.81 days.

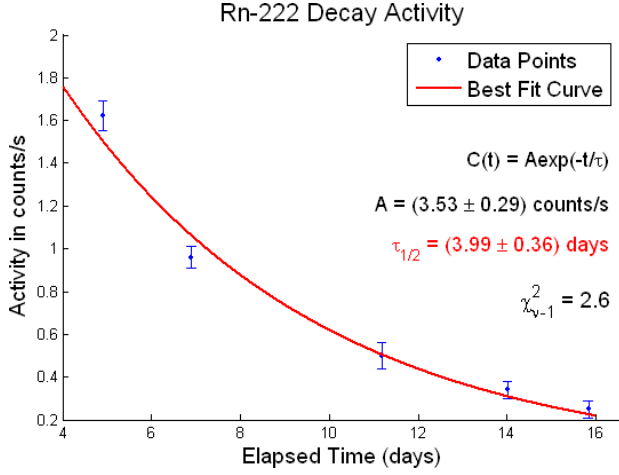


FIG. 5: Rise time of activity of Rn^{222} and its decay products in the liquid scintillator.

6.2. Po^{218} Half-Life Determination

Po^{218} is the direct decay product of Rn^{222} and therefore top of the decay chain as seen with the solid-state detector in the metal can. As such, we would expect to see Po^{218} decay exponentially. We observe the evolution of the Po^{218} peak in the can detector after we turn off the bias voltage (in effect, cutting off the replenishment of polonium atoms). This situation is complicated by the spread of each energy peak in the MCA. Oftentimes, the resolution is not high enough to distinguish between the Po^{218} , Bi^{212} , and Rn^{220} peaks. In order to separate the Po^{218} behavior from the other noise contributors, some manipulations were necessary.

Po^{212} is the short-lived daughter isotope ($\tau_{1/2} \mu s$) of the decay of Bi^{212} , and would very quickly equilibrate with its parent isotope and assume the activity of Bi^{212} . Since we are interested in finding the contribution of Bi^{212} , we take advantage of this parent-child relationship to remove this source of noise. The integral under the Po^{212} peak is subtracted from the peak of interest for each time slice.

To avoid transient behavior resulting from an incomplete stoppage of polonium influx, we allow a few minutes to pass before data is taken. Background is determined to be the average of the last seven data points taken. We give the overall fit in Figure 6. The best fit exponential gives a half-life for Po^{218} of 3.14 ± 0.33 minutes.

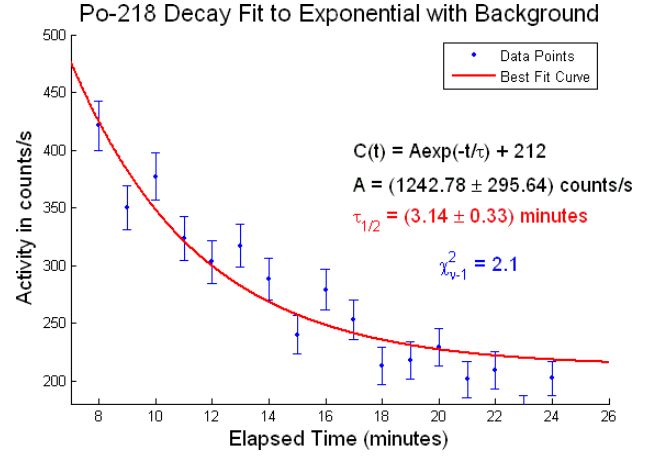
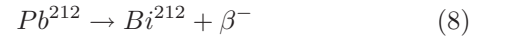
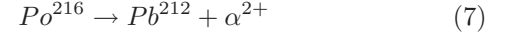


FIG. 6: Best fit curve for Po^{218} decay after Po^{212} subtraction. 20 second integration every minute.

6.3. Determination of Half-Life of Bi^{212} and Bi^{211}

Bismuth-212 is the product of two successive radioactive decays from polonium.



As a result, its expected behavior will not be quite as simple as that of the previous isotope. Instead, we must solve analytically the Bateman Equations described in Section 3 in order to generate the expected time-evolving functional form of its decay rate. Initial values can be determined by taking advantage of an equilibrium situation, in which all the decay rates in the chain must be identical. If we take A, B, and C to be the abundance of the individual isotopes, we derive from Equation 4.1 in [4] the following relation,

$$A/\tau_A = B/\tau_B = C/\tau_C \quad (9)$$

If we allow the setup to reach equilibrium and then switch off the voltage, A, B, and C become our initial abundance ratios for a Bateman fit. We use a tool created by Scott Sanders (a graduate T.A. in our lab) in order to generate the proper form. The zero time is shifted so that transient Po^{218} activity has essentially decayed away. We integrated for 15 minutes every 1.5 hours. Our results can be viewed in Figure 7, where we find the half-life of Bi^{212} to be 1.13 ± 0.13 hours.

In the same way, the half-life of Bi^{211} can be found. These results are shown in Figure 8.

6.4. Measurement of the Half-Life of Po^{212}

A Po^{212} atom is created with the emission of an electron. It very quickly decays producing an alpha particle and a Pb^{208} atom. In this portion of the lab we rely on

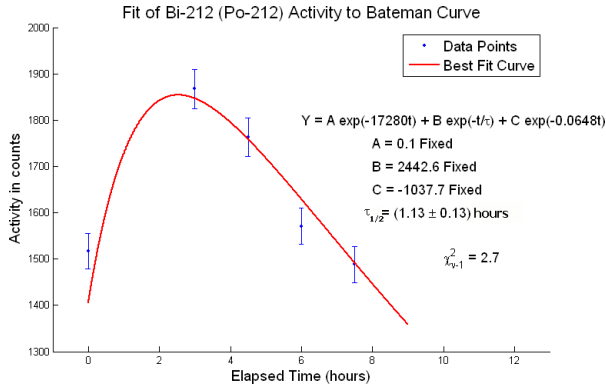


FIG. 7: Bi^{212} measured activity fit to the Bateman equations of decay.

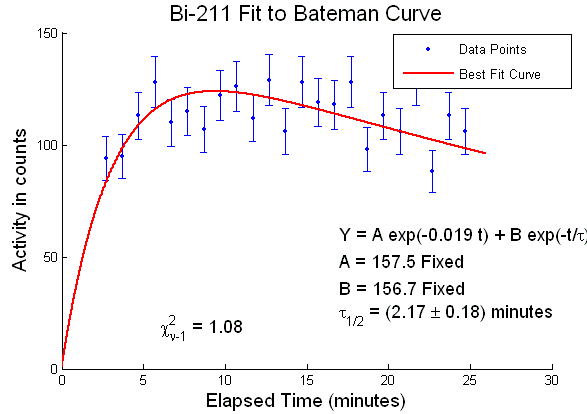


FIG. 8: Integration under the Bi^{211} peak for 20 seconds every minute yields the data shown here, fit by the Bateman equations governing its decay.

the near coincidence of these sequential events to record a distribution of the time intervals between many instances of these events. In a successful measurement, first, a beta particle is emitted and captured by the scintillator; the signal is sent to the START node on a time-to-amplitude converter (TAC). A short time later an alpha particle is emitted and recorded by the silicon detector; the signal is sent through a delay cable and finally connected to the STOP input on the TAC. The TAC translates the separation in time, t_0 , to an amplitude, $h_0 \propto t_0$, for use as input for the MCA.

Taken overnight, our raw data and best fit along with our half-life results are shown in Figure 9. We obtain a half-life of $\tau_{1/2} = 0.31 \pm 0.01 \mu s$. The error was determined as a combination of random error and the fluctuations in the half-life parameter as the left and right cut-offs were varied by several hundred bins.

6.5. Measurement of the Half-Life of Po^{214}

We return to the PMT coincidence circuit (and our sample of Rn^{222}) for the determination of the half-life

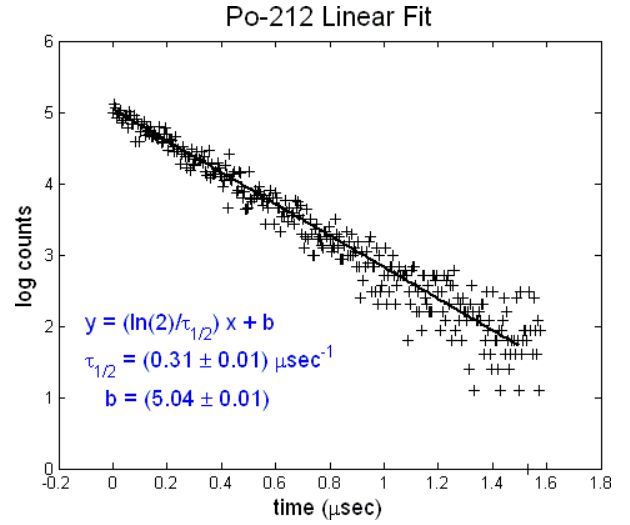


FIG. 9: A semi-log plot of our raw data on the half-life of Po^{212} and the linear best fit through this data.

of Po^{214} , which is significantly shorter than any of the half-lives found so far. We again connect our set up to a TAC and then to an MCA.

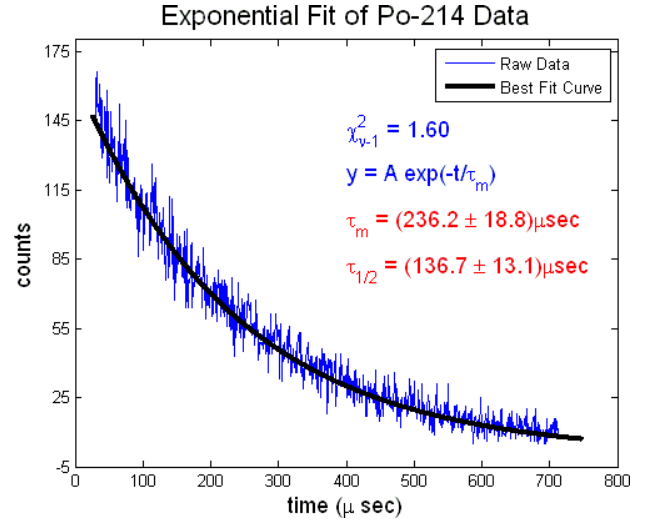


FIG. 10: Shown here is the raw data from the Po^{214} half-life experiment and the best fit through the data reduced by a running average manipulation.

In measuring the half-life of Po^{214} we seize the fact that it is the shortest lived isotope in the decay chain of Rn^{222} . By setting our maximum range on the TAC to be approximately 1 ms, we limit ourselves to accidentals and the two decay events that signal the creation and disintegration of a Po^{214} atom. The MCA was allowed to collect data for 4 days, the resulting curve fit an exponential with a $\chi^2_{\nu-1}$ of 1.6. It was determined that background noise was negligible (not observed in our data) so the curve was fit to a pure exponential, see Figure 10. The result for the half-life of Po^{214} was $163.7 \pm 13.1 \mu s$.

7. VERIFYING THE GEIGER-NUTTALL LAW

With an arsenal of isotope half-lives and energies in hand, we turn to our ultimate goal of assessing the linearity of the $\ln(1/\tau_{1/2})$ vs. Z/\sqrt{E} relationship. We fit the isotopes whose half-lives and energies we measured, and for verification, include also accepted values from a trusted database of various nuclides. The resulting graph is Figure 11, and we do indeed observe a strong linear relationship between the two stated parameters.

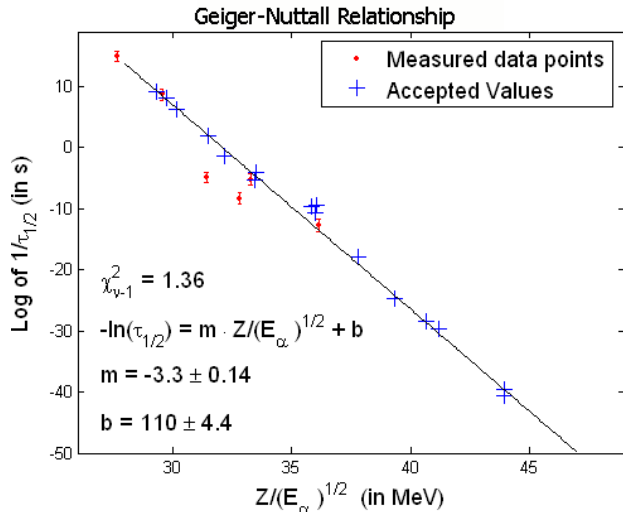


FIG. 11: Geiger-Nuttall Fit with measured values in red and additional accepted values in blue. Errors on energy were propagated to represent errors in half-life. Notice the bismuth outliers. They were omitted in the best fit in order to obtain representative parameters.

We were able to fit our data to the model predicted by quantum mechanics with a $\chi^2_{\nu-1}$ of 1.36. Convincingly, additional values determined outside of this experiment were also in good linear agreement with our results. We have seen strong evidence in favor of the theory of quantum tunneling.

8. ERROR ANALYSIS

Statistical error dominated our half-life observations. For the most part our measurements involved counting algorithms in which our raw data could be modeled roughly by Poisson probabilities, with $\sigma_\mu = \sqrt{A/N}$, where A is the measured value and N is the number of trials. Where there was obvious systematic error, we attempted to account for the bias using methods ranging from background/noise subtraction to observational interval adjustment to cut-off variation. For the most part accepted values were within one standard deviation of our half-life results.

Errors on energy are purely from calibration and were

determined easily using the error propagation formula. In general they were approximately 5% of the energy value due to the width of the peaks.

However, the premise of quite a few of our fits assumed equilibrium within the metal can. But this can only be determined with little certainty. Though we applied a continuous voltage for as long as we supervised the can, we were unable to verify for exactly how long a can had been charging prior to the beginning of our experiments since our set-up was needed equally by other lab sections. A lack of equilibrium would change the ratios of isotope abundances and alter our Bateman fits.

In addition we observed a peak-widening over a period of two-weeks in our MCA output. After a discussion with Dr. Scott Sewell, we concluded that this was due to a rapid degradation of the solid-state detectors. The result was increased difficulty in the resolution of our peaks, causing separate peaks to appear as one and complicating the extraction of necessary data.

Finally, we notice in our Geiger-Nuttall fit that not all isotopes fall perfectly along the same line. However, this is to be expected since Gamow's derivation of the theoretical relationship was calculated on the basis of an approximation. The constants cited in Equation 2 are not actual constants but depend to a small degree on parameters such as the mass number, atomic number, and atomic radius of the atom. More accurately, the Geiger-Nuttall relationship can be fit separately to each decay chain, each element, and so on, where useful information may be extracted.

9. CONCLUSIONS

By observing the alpha emission of several radioactive isotopes, we have qualitatively verified the Geiger-Nuttall relationship and aligned it with quantum mechanical models. Our results for the half-lives of each isotope is shown in the table following:

Element	Measurement	Measured $\tau_{1/2}$	Accepted $\tau_{1/2}$
^{212}Po	Si Detector + TAC	$0.31 \pm 0.01 \mu\text{sec}$	$0.299 \mu\text{sec}$
^{214}Po	Scint. + TAC	$163.7 \pm 13.1 \mu\text{sec}$	$164.4 \mu\text{sec}$
^{218}Po	Can Spectrum	$188.4 \pm 19.8 \text{ sec}$	186 sec
^{212}Bi	Can Spectrum*	$67.8 \pm 7.8 \text{ min}$	60.55 min
^{211}Bi	Can Spectrum*	$2.17 \pm 0.18 \text{ min}$	2.14 min
^{222}Rn	Scint.+ Counter	$3.86 \pm 0.41 \text{ days}$	3.8235 days

TABLE I:

It is evident that quantum mechanics has predictive powers on the atomic scale that classical mechanics lacks, and with this knowledge we are closer to understanding the true processes that govern the world around us.

-
- [1] Lim, Yung-Kuo, Problems and Solutions on Atomic...Physics, World Scientific. [2000]
 - [2] Baum, E., Nuclides and Isotopes, 16th Edition, Lockheed Martin. [2002]
 - [3] Table of Nuclides, <http://atom.kaeri.re.kr/>, Korea Atomic Energy Research Institute, [2000]
 - [4] Sewell, Quantum Mechanics of Alpha Decay, 8.13 Course Reader, [2007]

Acknowledgments

We are grateful of the assistance we received from the Junior Lab staff, for the assistance offered by Prof. Ulrich Becker and Dr. Scott Sewell in the set up of Po^{212} , and for the bateman function generating script provided by (almost Dr.) Scott Sanders.

All non-linear fits were made with the MATLAB scripts made available to us on the Junior Lab website: <http://web.mit.edu/8.13/www/jlmatlab.shtml>.